© 2015. Published by The Company of Biologists Ltd | The Journal of Experimental Biology (2015) 218, 1259-1269 doi:10.1242/jeb.117317

RESEARCH ARTICLE

Paracellular pathway remodeling enhances sodium secretion by teleost fish in hypersaline environments

Regina R. F. Cozzi, George N. Robertson, Melanie Spieker, Lauren N. Claus, Gabriella M. M. Zaparilla, Kelly L. Garrow and William S. Marshall*

ABSTRACT

In vertebrate salt-secreting epithelia, Na^+ moves passively down an electrochemical gradient via a paracellular pathway. We assessed how this pathway is modified to allow Na^+ secretion in hypersaline environments. Mummichogs (*Fundulus heteroclitus*) acclimated to hypersaline [2× seawater (2SW), 64‰] for 30 days developed invasive projections of accessory cells with an increased area of tight junctions, detected by punctate distribution of CFTR (cystic fibrosis transmembrane conductance regulator) immunofluorescence and transmission electron miscroscopy of the opercular epithelia, which form a gill-like tissue rich in ionocytes. Distribution of CFTR was not explained by membrane raft organization, because chlorpromazine (50 μmol l^{-1}) and filipin (1.5 μmol l^{-1}) did not affect opercular epithelia electrophysiology. Isolated opercular epithelia bathed in SW on the mucosal side had a transepithelial potential (V_t) of +40.1±0.9 mV (N=24), sufficient for passive Na^+ secretion (Nernst equilibrium voltage≡E_{Na}=+24.11 mV). Opercular epithelia from fish acclimated to 2SW and bathed in 2SW had higher V_t of +45.1±1.2 mV (N=24), sufficient for passive Na^+ secretion (E_{Na}=+40.74 mV), but with diminished net driving force. Bumetanide block of Cl^- secretion reduced V_t by 45% and 29% in SW and 2SW, respectively, a decrease in the driving force for Na^+ extrusion. Estimates of shunt conductance from epithelial conductance (G_t) versus short-circuit current (I_{sc}) plots (extrapolation to zero I_{sc}) suggested a reduction in total epithelial shunt conductance in 2SW-acclimated fish. In contrast, the morphological elaboration of tight junctions, leading to an increase in accessory-cell–ionocyte contact points, suggests an increase in local paracellular conductance, compensating for the diminished net driving force for Na^+ and allowing salt secretion, even in extreme salinities.

KEY WORDS: Tight junction, CFTR, Immunocytochemistry, Electrophysiology, *Fundulus heteroclitus*, Euryhaline, Teleost fish, Gill epithelium, Ionocyte, Chloride cell

INTRODUCTION

The mummichog (or common killifish) *Fundulus heteroclitus* is well known for its euryhaline capabilities, readily adapting to environments ranging from freshwater to hypersaline conditions as high as 120‰, 3.75× seawater (SW) (Griffith, 1974). Thus *F. heteroclitus* has been and continues to be an important model organism for understanding mechanisms of teleost osmoregulation, as documented in two major reviews. Karnaky (1986) focused on chloride cell structure and function in the ionocyte-rich opercular epithelium, while Wood and Marshall (1994) compared *in vitro* and *in vivo* approaches to understanding euryhalinity in teleost fishes. Recently, the species has been recognized as a valuable genomic model in physiology (Burnett et al., 2007; Whitehead, 2010; Whitehead et al., 2011a,b) and toxicology (Whitehead et al., 2012) and sequencing of the genome is complete (www.fundulus.org). Current models for teleost ion transport and acid–base regulation in gills (Evans et al., 2005) include transcellular Cl^- secondary active transport in a two-step process in seawater-type NaCl-secreting ionocytes [Type IV ionocytes as per functional classification (Hiroi et al., 2005)]. The opercular epithelium, an epithelium rich in ionocytes, is a valuable model for the operation of the main ion-secreting organ (the gills) that has contributed greatly to the understanding of ionocyte function (Karnaky and Kinter, 1977; Karnaky, 1986; Wood and Marshall, 1994). By this model, accumulation of intracellular Cl^- is by transmembrane entry across the basolateral membrane via the Na,K,2Cl cotransporter (NKCC1) (Haas and Forbush, 2000), followed by Cl^- exit down its electrochemical gradient via the cystic fibrosis transmembrane conductance regulator (CFTR) anion channels localized in the apical membrane. CFTR has been identified in ionocytes of the opercular epithelium (Marshall et al., 1995), the CFTR gene cloned from mummichogs (Singer et al., 1998, 2008), and in seawater fish the channel is present in the apical membrane of ionocytes (Hiroi et al., 2005; Marshall et al., 2002; McCormick et al., 2003; Tang and Lee, 2007). Adaptation to seawater augments ion secretion in parallel with increased CFTR expression (Marshall et al., 1999) and there is mobilization of both the CFTR and NKCC1 cotransporter in ionocytes, placing more of the former in apical membrane and more of the latter in the basolateral membrane (Marshall, 2002; Marshall et al., 2002). Hence Cl^- secretion is transcellular and depends on intracellular Cl^- activity and a favorable transmembrane potential across the apical membrane to drive Cl^- into the environment (SW or hypersaline). However, the intracellular Cl^- activity and electrical driving force across the apical membrane have not yet been measured.

The secretion of Na^+, the counter-ion to Cl^-, is also thought to proceed by passive transport, aided by the positive transepithelial voltage that is generated at least in part by the exit of Cl^- at the apical membrane. The location of the Na^+ leak pathway is between the ionocyte and accessory cells in the apical crypts where Cl^- exits. Cl^- efflux generates a 'loop current' where Cl^- exit carries current (of negative charge) out of the gill, while Na^+ paracellular exit carries the current back into the gill, completing the loop. To drive Na^+ efflux efficiently by a given transepithelial voltage, close juxtaposition of the two pathways is important to minimize stray electrical resistance; by Ohm's Law, excessive stray resistance in the circuit will otherwise limit the current flow, i.e. the rate of NaCl secretion.

Department of Biology, St Francis Xavier University, J. Bruce Brown Hall, Room 214, 2320 Notre Dame Avenue, Antigonish, Nova Scotia, Canada B2G 2W5.

*Author for correspondence (bmarshal@stfx.ca)

Received 26 November 2014; Accepted 23 February 2015

The Journal of Experimental Biology (2015) 218, 1259-1269 doi:10.1242/jeb.117317

NaCl secretion in seawater and hypersaline conditions

A morphologically-distinct cell type in eel gills, rich in mitochondria, was thought to be responsible for NaCl secretion by marine teleost gills and these cells were termed 'chloride-secreting cells' (Keys and Willmer, 1932). Philpott and Copeland (1963) recognized a field of these cells in the gills, skin and buccal epithelium of *F. heteroclitus* and described the curious ultrastructure, with elaborated basolateral membrane surface in serpentine tubules that formed a meshwork among the well-organized mitochondria. Na^+,K^+-ATPase, localized specifically on the basolateral membrane of these 'chloride cells' (Karnaky et al., 1976) displayed higher activity in the gills of *F. heteroclitus* adapted to seawater than in those adapted to freshwater (Epstein et al., 1967; Towle et al., 1977). Na^+,K^+-ATPase activity proved to be the indirect driving force for transcellular Cl^- exit from the animal into seawater (Silva et al., 1977a,b). Na^+,K^+-ATPase, which is responsible for producing the Na^+ transmembrane gradient that drives NKCC operation, has been cloned from *F. heteroclitus* (Semple et al., 2002). There is complex regulation of Na^+,K^+-ATPase at the protein and mRNA expression levels associated with adaptation to seawater (Choe et al., 2006; Mancera and McCormick, 2000; McCormick et al., 2009; Scott and Schulte, 2005). Tilapia (*Oreochromis mossambicus*) in hypersaline conditions significantly shift their gill proteome, featuring increased expression of mitochondrial proteins and the stress protein NDRG1 (Kültz et al., 2013). The Salton Sea, an endorheic lake in California (current salinity 44‰) has endemic fish populations of strongly euryhaline fish (Riedel et al., 2002) and responses to hypersalinity involve ionoregulatory responses primarily to gill and posterior intestine epithelia (reviewed by Laverty and Skadhauge, 2012). Whereas strongly euryhaline fish can survive indefinitely in salinities well above full-strength seawater (32‰), hypersaline conditions above 65‰ cause significant increases in plasma ions (Na^+ and Cl^-), loss of tissue water content and increased apoptosis in gill ionocytes of the strongly euryhaline tilapia hybrid (*Oreochromis mossambicus*× *O. urolepsis honorum*) (Sardella et al., 2004). Hypersaline conditions (2SW) evoke hypertrophy of ionocytes of pupfish gills, elaboration of the basolateral membrane surface area (*Cyprinodon variegatus*) and, in pupfish and mummichog gills, marked increases in basolateral Na^+,K^+-ATPase and enzyme activity (Karnaky et al., 1976). In sea bass (*Dicentrarchus labrax*), hypersalinity evokes ionocyte hypertrophy and increased accessory cell interdigitation with ionocytes, forming complex morphologies attributed as 'leaky junctions' (Varsamos et al., 2002). However, research is lacking on the effects of hypersalinity on the electrophysiology of passive transport components, CFTR and the paracellular pathway.

Paracellular pathway and Na^+ secretion

The tight junctions between ionocytes and accessory cells of seawater teleost fish gills are permeable to cations, even to La^{3+}, and form a localized cation-permeable pathway (Sardet et al., 1979; Scheffey et al., 1983) in an epithelium of pavement cells that are connected by deep, relatively impermeable tight junctions (Monteiro et al., 2010; Sardet et al., 1979). These permeable junctions balance the anion current emanating from the ionocyte and together comprise the total measurable epithelial conductance, as detected by vibrating probe experiments (Foskett and Machen, 1985). The mechanism of maintaining high cation permeability in intercellular junctions between ionocytes and accessory cells is not known. One possibility is that a special claudin junctional protein in these junctions imparts cation selectivity. Claudins are a complex family of intermembrane proteins in a large gene family with more than 30 members (Chasiotis et al., 2012). In smolting of Atlantic salmon, claudin 10e may be important in seawater acclimation and tight junction structure in the gill epithelium (Tipsmark et al., 2008a,b). Acclimation of tilapia (*O. mossambicus*) to seawater decreases transcript abundance of claudin-3 and claudin-4 junctional proteins (Tipsmark et al., 2008a,b), suggesting that cation permeability could actually rely on the selective lack of claudins in Na^+-permeable junctions rather than their extra presence. Acclimation of mummichogs to seawater and low salinity reveals lower transcript abundance of claudins 3 and 4 in gill epithelium in seawater (Whitehead et al., 2011a,b) and in the pufferfish *Tetraodon nigroviridis*, acclimation to seawater and hypersaline reduces gill transcript levels of claudin 3 (Bagherie-Lachidan et al., 2008). In cultured pavement cells from seawater pufferfish, claudin 6, claudin 10d and claudin 10e are absent, yet these are responsive to salinity change in whole gill epithelium where ionocytes are present (Bui et al., 2010). The cation permeability thus may reside in the protein make-up of the special junctions between ionocytes and accessory cells.

Transepithelial potentials measured *in vivo* in seawater teleost fish have long been recognized to approximate the Na^+ diffusion potential (Nernst equilibrium potential) (Potts, 1984) for most marine species tested, including *F. heteroclitus* (+18 mV), but there are several teleost fish species for which the potential is much lower, and, in some species, the opposite polarity (e.g. *Opsanus beta* with a V_t of −8 mV). For the fish with positive V_t, this voltage was thought to be the driving force for Na^+ secretion, such as in the model proposed (Silva et al., 1977a,b) for teleost fish gills and confirmed by vibrating probe studies of ionocytes (Foskett and Machen, 1985; Scheffey et al., 1983) and in ion flux experiments with voltage-clamped isolated opercular epithelia (Degnan and Zadunaisky, 1980). Thus for the symmetrical saline condition, Na^+ certainly has sufficient driving force to produce Na^+ secretion via the paracellular pathway. The potential measured was usually smaller than the calculated Nernst equilibrium potential for sodium (E_{Na}, approximately +25 mV in seawater fish), which is probably a result of the actual V_t being shunted by leak pathways, such as leakage around the catheter or physiological leakage represented by large surface areas of respiratory epithelium. Importantly, measurements made in preparations with the same salt-secretion mechanism but with much less shunt area, such as the yolk sac larvae of *F. heteroclitus* that is capable of seawater ion regulation yet has no gill area, gave results that were significantly higher than E_{Na}, thus demonstrating that in seawater there could be a voltage sufficient by itself to drive Na^+ secretion. Specifically, V_t measured across the yolk sac of *F. heteroclitus* embryos in seawater was +50±1.7 mV and +40±1.3 mV for *F. bermudae*, (Guggino, 1980), clearly higher than the E_{Na} of approximately +25 mV in seawater. The remaining question is whether there is sufficient driving force to secrete Na^+ in asymmetrical conditions, particularly in conditions of hypersaline exposure, conditions that are physiologically relevant to the fish in the environment.

In this study, we hypothesized that V_t should exceed E_{Na} in seawater and in hypersaline conditions and that ultrastructure should indicate changes in shunt structure in hypersaline conditions. To test these hypotheses, we acclimated adult *F. heteroclitus* to SW and 2SW and tested isolated opercular epithelia in Ussing chambers electrophysiologically to compare V_t with calculated E_{Na}, with SW or 2SW bathing the outside surface. We also found that there were clear differences in the ultrastructure and arrangement of intercellular junctions between accessory cells and ionocytes, featuring punctate CFTR distribution in ionocytes and multiple interdigitations of accessory cells with ionocytes. We estimated that

The Journal of Experimental Biology (2015) 218, 1259-1269 doi:10.1242/jeb.117317

the increased availability of junctions increases the efficiency (conductance) of the pathway such that, even with diminished voltage driving force in hypersaline conditions, Na^+ secretion would continue. Paradoxically, the overall conductance of the paracellular pathway, extrapolated from the linear relationship between short circuit current (I_{sc}) and epithelial conductance (G_t), decreases in 2SW, implying that the majority of tight junctions become tighter while a minority of junctions, those involved in Na^+ secretion, become more conductive.

RESULTS

Immunocytochemistry

CFTR was present in the opercular epithelia of killifish acclimated to SW and 2SW. Although all of the ionocytes showed immunofluorescence in the apical crypts, the distribution of the CFTR varied between the salinities. In epithelia of fish acclimated to SW, the majority of the apical crypts showed a continuous and diffuse distribution of CFTR, thus forming a fluorescent ring delineating each crypt (Fig. 1A–C). Although this type of distribution was also visible in epithelia of fish acclimated to 2SW, the majority of the apical crypts showed discontinuous fluorescence along the crypt ring, indicating that CFTR formed punctate (bright fluorescent dots surrounded by lower fluorescence, Fig. 1D–F). In fact, 78% of SW ionocytes contained diffuse CFTR in their apical crypts, while the rest (22%) had punctate CFTR distribution. In 2SW-acclimated fish, the number of apical crypts with diffuse CFTR significantly decreased to 25%, while the number of crypts containing CFTR nodes significantly increased to 75% (Fig. 2A). Also, apical crypts were significantly deeper in the SW ionocytes displaying diffuse CFTR (4.14 µm deep) compared with all other groups (2.6–3.1 µm deep) (Fig. 2B). Furthermore, for those apical crypts with condensed nodes, the number of dots per apical crypt was significantly higher in the 2SW epithelia compared with the SW epithelia (6.58±0.079 dots per apical crypt, N=12 animals, 106 crypts scored versus 5.08±0.152 dots per apical crypt, N=12 animals, 32 crypts scored, respectively; P<0.0001, unpaired t-test).

Electron microscopy

Transmission electron microscopy (TEM) revealed that the apical crypts of ionocytes of fish acclimated to 2SW had complex interdigitations of accessory cell processes and ionocyte processes alternating around the circumference of the apical crypt (Fig. 3), compared with the typical single projection of the accessory cell. In the figure, there are six patches of ionocyte membrane alternating with six sections of accessory cell in the apical portion of the ionocyte, the accessory cell projections are distinguishable because of their greater electron density. The junctions are simple and shallow (<0.5 µm), as is typical of accessory-cell–ionocyte junctions.

A diagrammatic rendering of the accessory-cell–ionocyte interaction (Fig. 4) indicates that processes from one accessory cell may interrupt CFTR distribution at multiple locations around the perimeter of the apical crypt. Our results did not show any evidence for multiple accessory cells (numerous nuclei adjacent to the ionocyte nucleus), but immunocytochemistry suggests the presence of only one accessory cell and the TEM data revealed multiple cell processes.

Electrophysiology

Membrane raft disruptors

Filipin, added at 1.53 µmol l^{-1} for 30 min had no effect on V_t (or the resting I_{sc}, not shown) and had no effect on the response of the opercular epithelia (OE) to hypotonic shock; control and test sets of membranes had large reductions in I_{sc} that were more than fully reversed with the reintroduction of isotonic Cortland's saline (Fig. 5A). Chlorpromazine, added at doses from 1.0 to 50 µmol l^{-1}, a dose sufficient to disrupt membrane rafts, had no significant effect on the spontaneous V_t (or I_{sc} not shown) of OE that were mounted *in vitro* in symmetrical saline (Fig. 5B).

Open-circuit voltages

Opercular epithelia from 2SW-acclimated fish had significantly higher V_t, +28% compared with SW-acclimated fish in symmetrical saline, which, in both cases, was substantially greater than E_{Na} (=0 mV). Perfusion of SW on the mucosal side increased V_t by 78% for SW and 48% for 2SW fish (Fig. 6) and the voltages were significantly higher than the calculated Nernst Equilibrium potential, E_{Na}, indicating that Na^+ net driving force would be inside to outside. Increasing the external salinity to 2SW for OE from fish acclimated to SW increased V_t a further 12% and the net driving force for Na^+ was still positive (Fig. 6). For fish acclimated to 2SW, the same manipulations resulted in a similar pattern. The

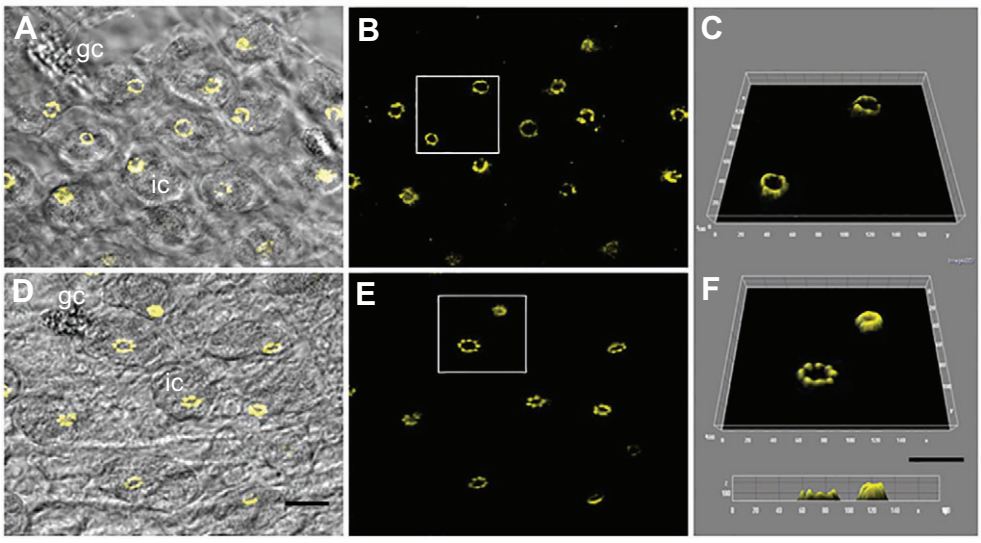

Fig. 1. CFTR immunofluorescence in ionocyte apical crypts of killifish. (A) In SW, the CFTR is evenly distributed in most of the apical crypts (yellow); ic, ionocyte; gc, granular cell. (B) Same frame as A without the brightfield view. (C) A magnified view displaying a 3D surface plot of the boxed region in B shows a continuous and diffuse distribution of CFTR in the apical crypts. (D) In 2SW, CFTR distribution is punctate in the majority of the apical crypts. (E) Same frame as D, without brightfield view, showing the variation in number of dots per apical crypt. (F) A 3D surface plot of the boxed region in D shows an apical crypt with punctate distribution of CFTR (presence of 8 dots), next to an apical crypt with diffuse CFTR. Below is an *x*–*z* scan of the two types of distributions. Scale bars: 10 µm.

The Journal of Experimental Biology (2015) 218, 1259-1269 doi:10.1242/jeb.117317

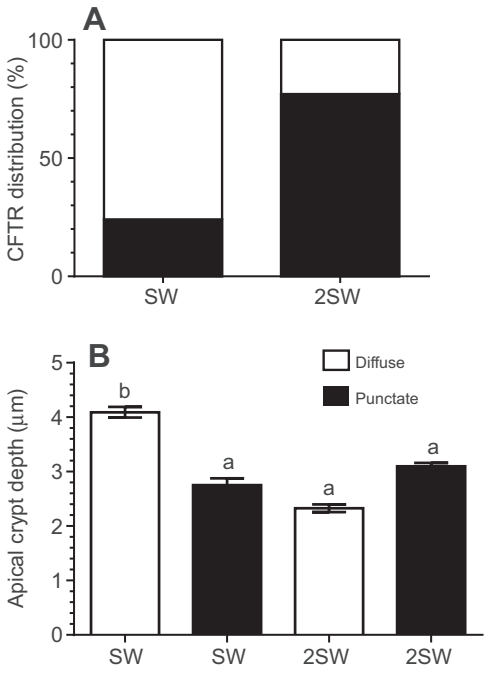

Fig. 2. Analysis of CFTR distribution in OE apical crypts of killifish acclimated to SW and 2SW. (A) In SW fish, 78% of the apical crypts showed a diffuse distribution of CFTR, whereas only 22% of the apical crypts had punctate CFTR. In 2SW, the CFTR distribution in the apical crypts was reversed, with a significant increase to 75% of punctate CFTR distribution, and a significant decrease to 25% of diffuse CFTR (P=0.0201, by Fisher's exact test, N=12). (B) Apical crypts were significantly deeper in ionocytes with diffuse CFTR from SW-acclimated fish compared with those with punctate CFTR, as well as both types of CFTR distribution in 2SW epithelia (differerent letters represent P<0.001, by one-way ANOVA and Bonferroni post test, N=12). Values are means±s.e.m.

OE from 2SW-acclimated fish had the high NaCl Cortland's saline to help mimic 2SW plasma. The calculated E_{Na} was thus slightly lower, but physiologically relevant. Overall, the Na^+ net driving force was positive for Na^+ efflux into SW and into 2SW.

Electrogenic Cl^- active transport was inhibited by two means: bumetanide, which blocks NKCC directly, and low K^+ Cortland's saline, which blocks NKCC by depriving the transporter of K^+ while simultaneously blocking Na^+,K^+-ATPase (Fig. 7). When Cl^- secretion was blocked by bumetanide, V_t decreased by 80% (−19 mV) in symmetrical Cortland's saline and with low-K^+ Cortland's saline bathing both sides of the OE, the decrease was 64% (−16 mV), thus reducing the driving force for Na^+. Perfusion of the mucosal sides with SW and 2SW increased V_t, as expected, but it was 45% lower than the SW control V_t and 29% lower than the 2SW control V_t. The measured V_t in asymmetrical conditions was less than the calculated E_{Na}. In the case of low-K^+ Cortland's with SW outside, there was a small (approx. +5 mV) V_t in excess of E_{Na}.

Similar manipulations were also performed on pieces of buccal epithelium, a membrane that has very few ionocytes and more mucus cells, compared with the OE. In symmetrical saline, the transepithelial resistance R_t was significantly higher (+280%) and this ratio constant with SW and with 2SW bathing the mucosal side; for both epithelia, higher salinity reduced R_t (Fig. 8A). The V_t measured across the buccal epithelium was significantly lower (63%) than the opercular epithelium in symmetrical saline, in SW (50%) and in 2SW (53% of opercular epithelium V_t) (Fig. 8B). For the buccal tissue, the net driving force for Na^+ was negative (less than E_{Na}), implying that if Na^+ were permeable at these locations, then net Na^+ movement would be not contribute to Na^+ secretion, rather the reverse would be true. The calculated I_{sc} for buccal epithelium in symmetrical saline was therefore much lower (22%) than that for the opercular epithelium, 45.4±11.0 (N=7) versus 205±21.5 μamp cm^{-2} (N=13), respectively.

Leak conductance

In the leak conductance estimate, initial I_{sc} of SW epithelia was 122±13.5 μamp cm^{-2} (N=11) and in 2SW epithelia was 137.8±14.1 (N=12), not significantly different (P=0.430, two tailed t-test). I_{sc} of SW epithelia after hypotonic shock was 31.0+4.7 μamp cm^{-2} (N=11) and in 2SW epithelia was 39.9±6.3 μamp cm^{-2} (N=12) and therefore not significantly different (P=0.310, two-tailed t-test). Individual plots of the hypotonic response as G_t versus I_{sc} extrapolated to I_{sc}=0 (y intercept) yielded leak conductance (G_L) estimates of 6.35±0.49 mS cm^{-2} for SW-acclimated opercular epithelia (N=11) and a significantly lower value (P<0.005, two-tailed t-test) of 3.74±0.40 mS cm^{-2} for 2SW-acclimated fish (N=12).

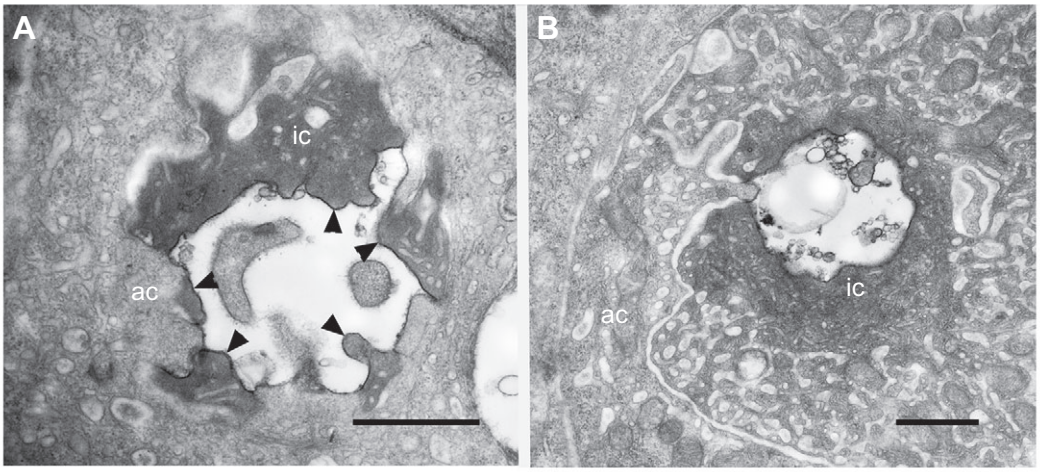

Fig. 3. Junctional complexes between ionocytes and accessory cells. Transmission electron micrograph in the plane parallel to the epithelial surface at the level of the apical crypt of an ionocyte (ic) with accessory cell (ac) in an OE from a 2SW-acclimated fish (A) and a SW-acclimated fish (B). The accessory cell processes (relatively electron-lucent) alternate with ionocyte apical membrane (relatively electron dense; arrowheads in A). Junctions between ionocyte and accessory cell processes are shallow. Scale bars: 1 μm.

The Journal of Experimental Biology (2015) 218, 1259-1269 doi:10.1242/jeb.117317

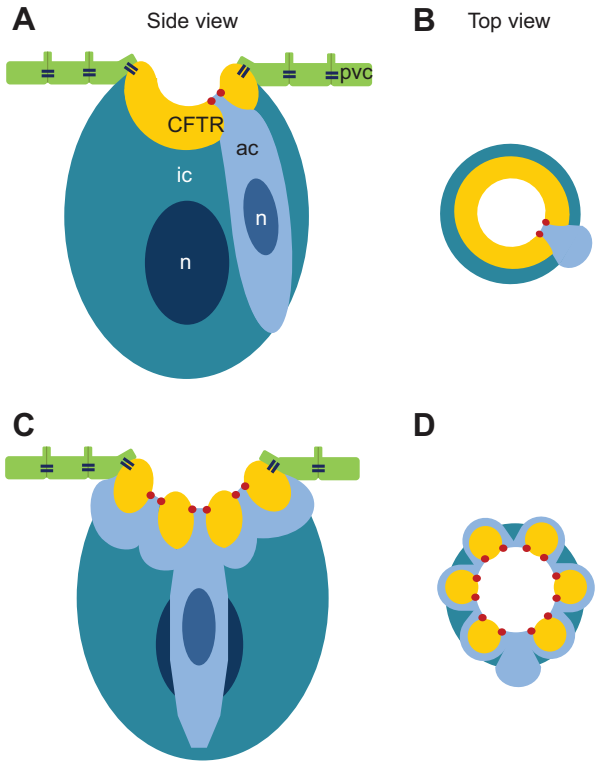

Fig. 4. Diagram of multicellular complexes formed in 2SW between ionocytes and accessory cells. (A) Side elevation of an ionocyte attached to one accessory cell by shallow tight junctions (red dots). CFTR immunofluorescence is diffuse and located throughout the apical crypt (yellow) except for the one area occupied by the accessory cell resulting in the absence of fluorescence. (B) Top view of A. (C) Side elevation of an ionocyte attached to an accessory cell with six processes with shallow junctions, typical of 2SW-acclimated fish. CFTR distribution is concentrated into punctate dots as a result of the apical interdigitation of the accessory cells into the crypt. (D) Top view of C. ic, ionocyte; ac, accessory cell; pvc, pavement cell; n, nucleus; red dot, shallow tight junctions; blue paired lines, long tight junctions.

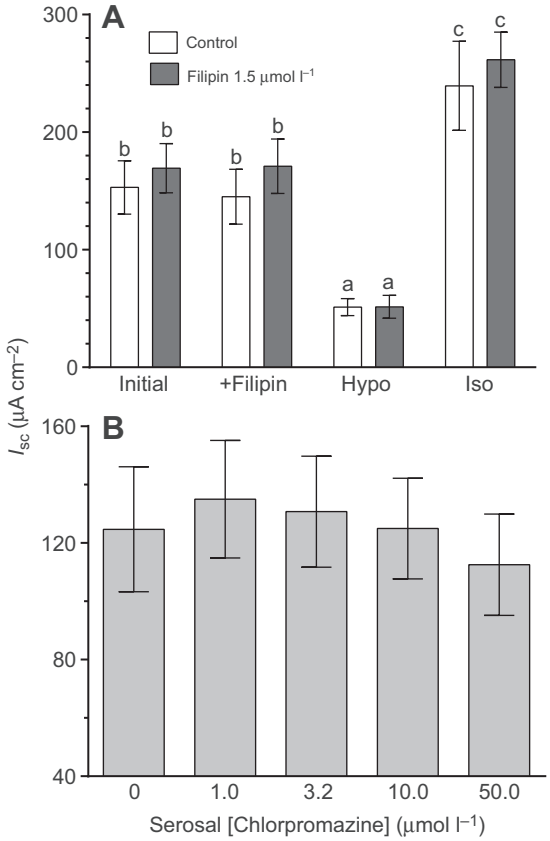

Fig. 5. Effect of raft-disrupting agents. Neither of the membrane-raft-disrupting agents (A) Filipin (1.5 µmol l^{-1}) or (B) Chlorpromazine (1–50 µmol l^{-1}) significantly affected the short-circuit current (I_{sc}) of OE. In addition, Filipin did not affect inhibition by hypotonic shock (Hypo) or the recovery on return to isotonic conditions (Iso); in both cases, hypotonic shock significantly inhibited I_{sc} and rebounded on return to isotonic conditions. Values are means±s.e.m. Different letters represent $P<0.001$.

Plasma ions and osmolality

Compared with controls in SW, acclimation to 2SW significantly increased plasma osmolality, from 356.5±2.11 to 378.7±4.27 mOsm kg^{-1} ($P<0.001$, $N=13$) and plasma Na^+ from 170.4±2.42 to 178.8±3.13 mmol l^{-1} ($P<0.05$, $N=13$), while there was no change in plasma K^+ in SW (5.747±0.23 mmol l^{-1}) or 2SW (5.790±0.18 mmol l^{-1}; $P=0.89$, $N=12$).

DISCUSSION

The main focus of this paper is to demonstrate that elaboration of the special leaky intercellular junctions between ionocytes and accessory cells is a necessary process to maintain conditions favorable for Na^+ secretion in a passive transport process. The elaboration is clear in that the distribution of CFTR immunofluorescence in the apical crypts of ionocytes is more often punctate in hypersaline conditions. The large number of loci for Na^+ secretion are thus close (about 1 µm or less) to the CFTR-rich zones, where there is secretion of Cl^-. The close juxtaposition of Na^+ and Cl^- secretion areas will reduce stray electrical resistance and enhance the coupling between the two ion-transport systems.

CFTR redistribution in hypersaline water

Acclimation of mummichogs to hypersaline conditions significantly alters the distribution of CFTR in the apical membranes of ionocytes in the OE. The ionocytes develop punctate CFTR distribution, detected by immunocytochemistry, in a ring around the apical crypt. Thus the junctions between accessory cells and ionocytes were more numerous in 2SW. In SW, CFTR distribution was restricted to the apical crypt and CFTR occupied all the membrane surface, except where the accessory cell interacts with the ionocyte to form a leaky junctional pathway. This is true for the OE of mummichogs where CFTR immunofluorescence was found to redistribute from sub-apical zones into the apical membrane by 24–48 h after transfer of FW-acclimated fish to SW (Marshall et al., 2002). We observed an increase in the number and complexity of accessory-cell–ionocyte interactions that were significantly more elaborate in hypersaline conditions. By transmission electron microscopy, sections through the apical crypts of ionocytes from mummichogs acclimated to hypersaline conditions revealed multiple loci of ionocytes alternating with cellular processes of accessory cells and these were loosely connected by intercellular junctions. Punctate distribution of apical CFTR immunofluorescence was observed previously in seawater-adapted Hawaiian goby ionocytes in the gill interlamellar region (McCormick et al., 2003).

Interdigitations with accessory cells

Accessory cells are small Na^+,K^+-ATPase-poor cells loosely attached to mitochondrion-rich chloride-secreting cells (Hootman and Philpott, 1980) and the junctions are permeable to cations

The Journal of Experimental Biology (2015) 218, 1259-1269 doi:10.1242/jeb.117317

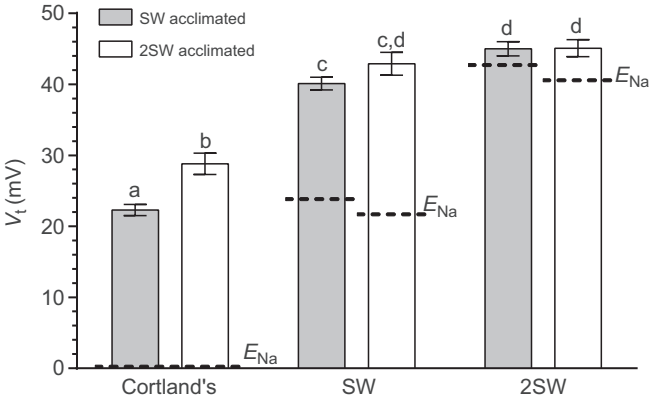

Fig. 6. Open-circuit V_t (corrected for junction potentials) for opercular epithelia from SW- and 2SW-acclimated killifish. OE were bathed in symmetrical Cortland's saline (Cortland's) or asymmetrically with seawater (SW) or twice seawater (2SW) on the mucosal side and compared with the calculated Nernst equilibrium potential, E_{Na}, for each asymmetrical condition (E_{Na}=0 for symmetrical conditions). The measured transepithelial potential, V_t, is higher than E_{Na} in all cases but this difference, the net driving force for Na^+ secretion, is markedly diminished in 2SW conditions. Values are means± s.e.m. Different letters represent P<0.001.

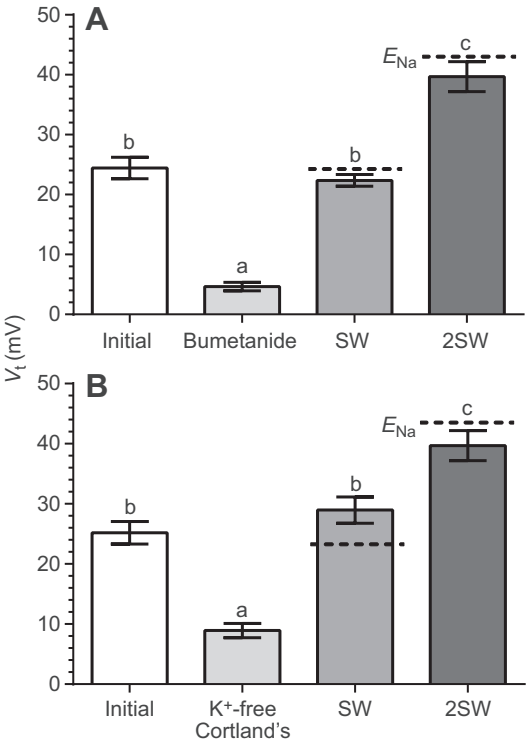

Fig. 7. Open-circuit V_t measurements in opercular epithelia from SW-acclimated killifish treated with bumetanide or K^+-free Cortland's saline to inhibit electrogenic Cl^- secretion. Either (A) bumetanide (0.1 mmol l^{-1}, serosal side) or (B) K^+-free Cortland's saline (serosal side) was used to inhibit electrogenic Cl^- secretion. Both treatments significantly inhibited V_t, while subsequent addition of SW and 2SW to the mucosal side increased V_t but not to the level of E_{Na} (dotted lines) (except for SW condition with K^+-free Cortland's, where K^+ reverse gradient would tend to increase V_t). Thus with electrogenic Cl^- secretion blocked, Na^+ secretion would slow down or reverse. Values are means±s.e.m. Different letters represent P<0.001.

including lanthanum (Sardet et al., 1979). There is evidence that ionocyte morphology can change quickly; transfer of larval Ayu (*Plecoglossus altivelis*) yielded interdigitation of ionocytes and accessory cells within 1–3 h of transfer, as detected by TEM (Hwang and Hirano, 1985). Accessory-cell–ionocyte junctions are dynamic, because OE from mummichogs acclimated to 1% SW rapidly (~45 min) respond *in vitro* to external isotonic saline by opening of the junctions to the SW-like conformation (Karnaky, 1991). Multicellular ionocyte–accessory-cell complexes, detected by TEM, are present in gill epithelium of Nile tilapia (*O. niloticus*) that were slowly acclimated to full-strength seawater (a salinity that is near their maximum) (Cioni et al., 1991) and similar multicellular alternating interdigitation structures were observed in SW-acclimated *O. mossambicus* gills (Shiraishi et al., 1997) and in sea bass (Varsamos et al., 2002). In the yolk sac epithelium of tilapia (*O. mossambicus*) transferred to seawater, the CFTR apical distribution was punctate and had multiple (up to 9) intense immunopositive concentrations arranged in a ring at the apical membrane (Hiroi et al., 2005). The authors interpreted the punctate distribution as processes of the ionocytes and accessory cells arranged alternately and interdigitated; they speculated that these could be multiple loci for paracellular Na^+ secretion. Transfer of FW-acclimated *O. mossambicus* to SW likewise redistributed CFTR into the apical membrane of type IV ionocytes, and some of the CFTR distribution was distinctly punctate, with 7–9 immunopositive dots surrounding the apical crypt wall (Hiroi et al., 2005). They speculated that the development and degeneration of the interdigitation between ionocytes and accessory cells occurs reversibly in parallel with the appearance and disappearance of CFTR at the apical membrane of ionocytes. Acclimation of hybrid salinity-tolerant tilapia to hypersaline conditions evoked more interdigitation of accessory cells and ionocytes in gill epithelium and apparent proliferation of accessory cells relative to ionocytes (Sardella et al., 2004) but at extremely high salinity (75‰ and above), many of the ionocytes become covered over by pavement cells, interpreted as an attempt to seal off permeable junctions against excessive salt gain. Our findings confirm morphologically the punctate distribution of CFTR in apical membranes of ionocytes of seawater teleost fish gills and the interdigitation of ionocytes and accessory cells. We offer a functional explanation that the close juxtaposition and increased number of Na^+-permeable paracellular pathways offers a low-resistance pathway for Na^+ secretion so that a modest transjunctional voltage gradient can drive Na^+ efflux through these junctions.

Functional interpretation

To reveal the functional significance of the morphological change to punctate CFTR distribution, we measured the transepithelial voltage and conductance *in vitro* with SW and 2SW bathing the external surface and found significant increases in V_t with SW and 2SW, averaging +45 mV. Previous investigations suggest that the interdigitations are associated with Na^+ paracellular transport (Hiroi et al., 2005) and could comprise 'leaky junctions' (Varsamos et al., 2002). Assuming that each point of contact between the accessory cell and ionocyte has the same conductance, most cells in SW have only two such contacts, whereas the 2SW fish would have 14, representing a 7-fold higher local conductance. To secrete Na^+, the measured voltage should exceed the Nernst equilibrium potential for Na^+ (E_{Na}) in all conditions, even in hypersaline solutions. We found this to be true: for SW and 2SW bathing the outer surface the measured V_t exceeded the calculated E_{Na}, demonstrating that the paracellular pathway Na^+ secretion is feasible and likely, even in 2SW. The maximal V_t we observed in 2SW was +52 mV and 25% (6 of 24 epithelia) generated V_t above +50 mV. Indeed, in mummichog larvae

The Journal of Experimental Biology (2015) 218, 1259-1269 doi:10.1242/jeb.117317

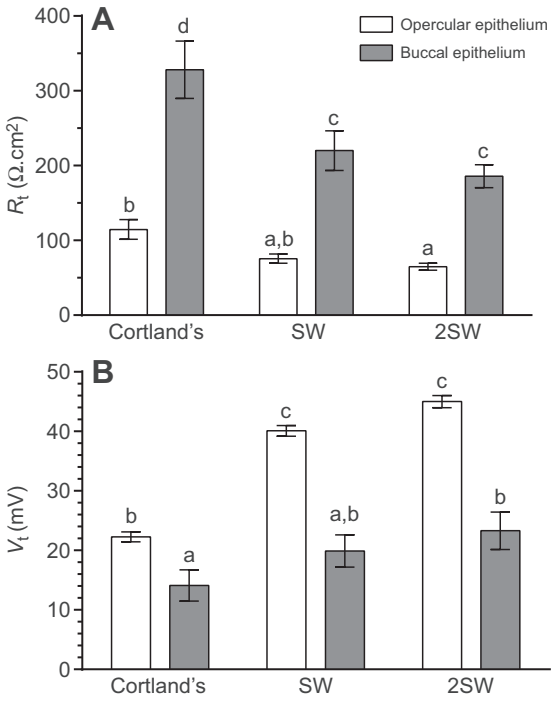

Fig. 8. Comparison of opercular epithelium (*N*=13) with buccal epithelium (*N*=7) in symmetrical Cortland's saline and with SW or 2SW on the mucosal side. Buccal epithelium had higher epithelial resistance R_t (A) and lower V_t (B) in symmetrical saline and significantly lower V_t than the calculated E_{Na} or the measured V_t of opercular epithelium in SW and 2SW, suggesting that the buccal epithelium would not contribute to Na^+ secretion in either SW or 2SW. Values are means±s.e.m. Different letters represent $P<0.001$.

in SW, the yolk sac membrane, rich in ionocytes and without the shunt formed by lamellae or edge damage, develops a V_t of +50±1.7 mV (Guggino, 1980), so this value may be close to the upper limit that these salt-secreting systems can develop. In extremely high salinities of 95‰, Tilapia have elevated plasma Na^+ to 260 mmol l^{-1} (Sardella et al., 2008); the calculated E_{Na} of +44.3 mV suggests that fish are forced to adjust their plasma Na^+ upward, so that the maximal V_t can still produce Na^+ secretion via the paracellular pathway. In contrast, we found that the buccal epithelium, which has few ionocytes, develops much lower V_t and I_{sc}, which confirms previous findings (Karnaky, 1980), but we predict that buccal epithelium would not contribute to Na^+ secretion in SW or 2SW. In conclusion, 3SW appears to be the maximum salinity for this type of salt secretion mechanism: +50 mV is close to the upper limit voltage and elaboration of tight junctions provides a high conductance paracellular pathway.

Another possible explanation of punctate CFTR distribution could come from membrane raft organization. CFTR anion channels are mobile in the plasma membrane and this mobility is impaired by the raft-disrupting agent filipin (Haggie et al., 2004). Disruption of formation of clathrin-coated vesicles inhibits the internalization of CFTR from the plasma membrane, resulting in an increase in the steady-state levels of cell-surface CFTR (Bradbury et al., 1999). Also, treating the thick ascending loop of Henle renal cells with chlorpromazine and filipin inhibits the rate of NKCC2 endocytosis (Ares and Ortiz, 2012). We tested for sensitivity of ion transport and its regulation using these two raft inhibitors, which inhibit clathrin-coated endocytosis. In neither case did we detect changes in transport rates or loss of sensitivity of the ion transport to osmotic (hypotonic) shock, where we would have expected increases in baseline NaCl secretion and a loss of responsiveness to hypotonic shock if endocytosis had been effectively disrupted. Although high concentrations of the drugs could possibly produce greater effects, the doses used were higher than most mammalian membrane raft experiments to date. We see no evidence that membrane rafts are the main mechanism to maintain Na^+ transport rate or CFTR distribution in hypersaline conditions. The source of structural stability of these interdigitations is unclear, but our unsuccessful preliminary experiments with disrupting agents suggest that membrane rafts are probably not the main stabilizing force. Traditional cytoskeletal-stabilizing structures are a possibility.

V_t compared with E_{Na}

Trans-gill potentials (TEPs) measured *in vivo* with full-strength seawater generally are smaller than the E_{Na} for most marine fish (Potts, 1984). For example, in *F. heteroclitus*, TEP was +18–23 mV, while the calculated E_{Na} was +28 mV (Pic, 1978). It is well known that stress-generated catecholamines are potent inhibitors of active Cl^- secretion in OE (Degnan et al., 1977; Foskett et al., 1982; Marshall and Bern, 1980) and this approach is a way of estimating the electrogenic component of the measured voltage, suggesting that 21 mV of the total TEP was electrogenic. Recently, confirming these estimates, TEP measured in SW for adult mummichogs was found to be +23 mV compared with the Nernst E_{Na} of +29.1 mV (Wood and Grosell, 2008). The authors concluded that the TEP in SW was dependent on open paracellular pathways and they estimated that at least 1/3 of the TEP was electrogenic; however, this study did not examine hypersaline conditions.

The *in vitro* mummichog OE bathed in symmetrical saline develops a V_t of 15–30 mV, a transepithelial potential that is strongly inhibited by addition of the α-adrenergic agonist clonidine (Marshall et al., 1993) and by the loop diuretics furosemide and bumetanide (Degnan et al., 1977; Eriksson and Wistrand, 1986) and here V_t might be taken as being mostly electrogenic, in that full inhibition in symmetrical saline brings the V_t close to zero. In these conditions, Na^+ influx and efflux respond to voltage clamping (+ and −25 mV) and conform to the predicted flux ratio equation, all indicating that Na^+ moves through a single barrier to Na^+ diffusion (Degnan and Zadunaisky, 1980). Furthermore, 1,3,5-triamino pyridine (TAP, 10 mmol l^{-1}) inhibited Na^+ and urea fluxes and decreased total epithelial conductance by 70–80% (Degnan and Zadunaisky, 1980), demonstrating that blockade of paracellular junctions by TAP blocks Na^+ permeation. Conversely, low pH (pH 3.9–4.0, a mimic of acid rain exposure) increased both epithelial conductance and Na^+ and mannitol fluxes, indicative of opening of a paracellular pathway to solute permeation in brook trout opercular epithelium (Marshall, 1985). There is general agreement that in symmetrical saline, Na^+ is passively distributed across these epithelia, in which Na^+ responds to changes in the voltage gradient in a manner predicted by the Ussing flux ratio equation that describes diffusion across a simple barrier. Structurally, there is also general agreement that Na^+ movement is via a simple cation-selective barrier, most likely the simple tight junctions between accessory cells and ionocytes. Meanwhile, active Cl^- secretion does contribute to the electrogenic portion of the measured V_t and in asymmetrical conditions may be a smaller component of the measured V_t. Based on *in vitro* TEP measurements in a variety of species, Fletcher argued that while variation in Na^+ efflux was close to that predicted by free diffusion responding to V_t, he concludes that some active secretion component is needed to explain the Na^+ flux ratio in seawater (Fletcher, 1977). In contrast, ion substitution and flux studies of opercular epithelium, Degnan (1984) concluded that there appeared to be a 1:1 coupling between transepithelial Na^+ and Cl^- transport.

The Journal of Experimental Biology (2015) 218, 1259-1269 doi:10.1242/jeb.117317

Estimates of shunt conductance

One measure of shunt conductance is extrapolation of I_{sc} versus G_t plots to zero I_{sc}. Assuming that the complete removal of the conductance associated with the transcellular active transport (as I_{sc}) would leave the net conductance of other presumably passive pathways. Assuming also that in mounting epithelia in Ussing-style membrane apertures produces minimal 'edge' damage, the residual conductance would approximate the sum of all the remaining intercellular junctions. The fact that we measure a lower shunt conductance in 2SW acclimated fish, compared with SW-acclimated fish, suggests that most passive pathways in the epithelium have less-permeable junctions in 2SW. This result confirms previous findings in opercular epithelium of *O. mossambicus* (Kültz and Onken, 1993). Also, cultured pavement cells from SW-acclimated sea bass *Dicentrarchus labrax* have lower transepithelial conductance (Avella et al., 1999) than in similar pavement cell cultures from freshwater fish, such as rainbow trout (Wood et al., 1998), tilapia (Kelly and Wood, 2002) and goldfish (Chasiotis and Kelly, 2011). Finally, the gill and skin epithelia have different patterns of claudin 27a and claudin 27c mRNA abundance with salinity acclimation, suggesting differential junctional permeability between typical pavement cell junctions and the ionocyte–accessory-cell junctions (Bagherie-Lachidan et al., 2009). To reconcile the apparent paradox of observing more-leaky Na^+ junctions localized near ionocytes, yet lower overall shunt conductance for the whole system, we infer that while the Na^+-permeable pathways increase in their conductance and restructure themselves to be nearer the anion pathway, simultaneously, the other tight junctions across the general surface of the epithelium, namely between pavement cells, become much tighter, presumably to minimize ion permeation from hypersaline solutions into the animal. The prediction from vibrating probe experiments is that the ionocytes of opercular epithelium of SW-acclimated tilapia comprise all of the tissue conductance except for 0.5 mS cm^{-2} and that most of that residual conductance may be an artifact of edge damage in Ussing chamber studies (Foskett and Machen, 1985) leaving a shunt (pavement cell junction) conductance near zero. More recently, the scanning ion selective electrode technique (SIET) has been applied to ionocytes in yolk sac membrane of seawater medaka embryos, and while ionocyte complexes (with accessory cells) had approximately equal Na^+ and Cl^- currents, single ionocytes had a Cl^- current but lacked a Na^+ current (Shen et al., 2011). Consistent with this interpretation, our results with the mummichog buccal epithelium, a structure similar to the OE but with fewer ionocyte and accessory cells (Karnaky, 1980), suggests that the Na^+ shunt conductance varies with the density of ionocyte complexes.

MATERIALS AND METHODS

Animals

Adult killifish (*Fundulus heteroclitus* Linnaeus 1766) of both sexes were trapped in Jimtown estuary, Antigonish, NS, and transported in coolers containing estuary water to the St Francis Xavier University Animal Care Facility. The fish were placed in full-strength seawater (32.0‰ salinity) in 450 l recirculating tanks at room temperature (20±1°C), adjusted to an ambient photoperiod under artificial lighting and were held for several weeks prior to experimentation. Approximately 40 fish were acclimated for at least 4 weeks to hypersaline conditions of 2SW (64‰ salinity), made hypersaline by addition of artificial sea salt (Instant Ocean, Blacksburg, VA, USA) to seawater. Fish were fed adjusted amounts of Nutrafin flakes (R.C. Hagen, Montreal, QC, Canada) twice daily to provide each fish with 1.0 g of food daily per 100 g of body weight. Fish were also fed meal-worms (*Tenebrio molitor*) 3 days a week. Fish were anesthetized in 1.0 g l^{-1} tricaine methane sulfonate (buffered to neutral pH) and were killed by pithing. The tail region was dried and blood was collected from razor-severed caudal vessels in heparinized capillary tubes, centrifuged immediately at 2000 ***g*** for 2 min and plasma frozen in microcentrifuge tubes for ion composition and osmolality. Opercular epithelia were dissected and bathed in modified Cortland's saline (composition in mmol l^{-1}: NaCl 159.9, KCl 2.55, $CaCl_2$ 1.56, $MgSO_4$ 0.93, NaH_2PO_4 2.97, $NaHCO_3$ 17.85 and glucose 5.55, pH 7.7–7.8 when bubbled with a 99%:1% O_2:CO_2 gas mixture, osmolality 317 mOsm kg^{-1}). For 2SW-acclimated fish, a high-NaCl Cortland's saline was used: regular Cortland's supplemented with 15.0 mmol l^{-1} extra NaCl (osmolality 334 mOsm kg^{-1}). To inhibit NaCl secretion, a K^+-free version of Cortland's saline was used: regular Cortland's without KCl but with 2.55 mmol l^{-1} NaCl extra (osmolality 316 mOsm kg^{-1}).

Immunocytochemistry

OE were dissected without the dermal chromatophore layer and pinned to modeler's sheet wax. Preparations were rinsed three times in rinsing buffer comprising 0.1% bovine serum albumin (BSA) in 0.05% Tween 20 in phosphate-buffered saline (TPBS) (composition in mmol l^{-1}: NaCl 137, KCl 2.7, Na_2HPO_4 4.3, and KH_2PO_4 1.4 at pH 7.4). The membranes were fixed for 2 h at −20°C in 80% methanol, 20% DMSO, then rinsed and immersed in a blocking solution with 5% normal goat serum (NGS), 0.1% BSA, 0.2% NaN_3 in TPBS, pH 7.4 for 30 min at room temperature in the dark. The membranes were then incubated in the primary anti-CFTR antibody (10 µg ml^{-1} in blocking solution) at 4°C overnight. Membranes were then rinsed three times and exposed to the secondary antibody (8 µg ml^{-1} in blocking solution) for 4 h at room temperature in the dark. After three final rinses, the membranes were mounted in mounting medium (Geltol; Immunon Thermo Shandon, Pittsburgh, PA, USA). Slides were viewed in single blind fashion and images were collected with a laser scanning confocal microscope (Olympus, Markham, ON, Canada; model FV300). In each OE, randomly selected *Z*-stack series were collected using a ×40 water objective (NA 1.15W), zoom of 3.0 and with optical sections of 0.50± 0.02 µm. An average of 35 sections was collected for each image. Perspective 3D surface plots were obtained using the Fiji image processing program. Apical crypt measurements (depths, CFTR and node distributions) were calculated in single blind fashion; non-adjacent areas were selected at random and apical crypts visible within this area were scored, excluding those touching the top and right borders.

Antibodies

Primary antibody used for detection of killifish CFTR was mouse monoclonal anti-human CFTR (R&D Systems, Minneapolis, MN, USA) with the epitope at the C-terminus, a zone that is conserved in killifish to human (Singer et al., 2008) and therefore is selective for this protein (Marshall et al., 2002; Robertson and Hazel, 1999). The secondary antibody used for immunofluorescence microscopy was goat anti-mouse immunoglobulin (IgG) conjugated with Alexa Fluor 488 (Molecular Probes, Eugene, OR, USA). Negative controls were performed by omitting the primary antibody.

Electron microscopy

Dissected OE were pinned flat to a wax square and immersion fixed for 1 h in a solution of 2% formaldehyde, 2% glutaraldehyde in 0.1 mol l^{-1} phosphate buffer, pH 7.4. The tissue was transferred to a glass vial, containing the same fixative, and stored overnight at 4°C. The fixative was rinsed out by two changes of phosphate buffer followed by one change of 0.1 mol l^{-1} sodium cacodylate (10 min per change). This was followed by immersion in a solution of 1% osmium tetroxide and 0.0015% Ruthenium Red in distilled water for 1 h. Ruthenium Red (740 molecular mass) bears six positive charges and stains the cell surfaces but does not cross the plasma membrane to the cellular interior (Chambers, 1973). The tissue was then rinsed with distilled water (2×10 min per change) and kept at 4°C for 4 days, after which it was stained *en bloc* in saturated aqueous uranyl acetate for 1 hour then dehydrated through an ascending series of ethanol. The ethanol was replaced by two changes of propylene oxide (10 min each) and the tissue was then slowly infiltrated with epoxy resin (EMBed-812, EMS,

Hatfield, PA, USA), placed in flat rectangular wells, and cured at 60°C for 2 days.

Thick sections (1 µm) were cut, parallel to the apical face of the operculum, and stained with Toluidine Blue until tissue was encountered. The blocks were then thin sectioned (100 nm) on a Reichert microtome and the sections stained with uranyl acetate (1 h) and lead citrate (4 min) for viewing on a Philips 410 transmission electron microscope. Digital images were captured using a SIA L12C digital camera and adjusted for contrast and brightness using Adobe Photoshop.

Electrophysiology using Ussing chambers

Opercular epithelia (OE) and sections of buccal epithelium from the roof of the buccal cavity were dissected and placed in Cortland's saline solution and placed over a nylon mesh and pinned onto a Plexiglas® disk with six insect pins around the 0.125 cm^2 central aperture. The OE or buccal epithelium was placed mucosal side up and gently stretched over the pins to hold it in place; silicone grease (Dow Corning High Vacuum) was thinly applied to both surfaces to ensure electrical isolation. The chambers were assembled and the two hemi-chambers simultaneously filled with Cortland's saline solution (symmetrical saline condition). The Ussing chamber water jacket temperature was adjusted using a controlled-temperature bath-circulator (Polyscience, Niles, IL, USA), permitting temperature control inside the chambers at 20±0.1°C. Chambers were connected to a current voltage clamp (D. Lee Co., Sunnyvale, CA) and two separate circuits were connected. Transepithelial potential difference (V_t; mV) was measured continuously; pulses of current (ΔI=10 µA) were delivered 1.0 s once per minute, producing voltage transients (ΔV_t) and allowing calculation of OE resistance (R_t=$\Delta V_t/\Delta I$×0.125 Ω cm^2) and OE current (I_{sc}=V_t/R µA cm^{-2}); output was recorded (iWorx® data recorder) with LabScribe® software. The I_{sc} has been shown to be equivalent to the net tracer flux of Cl^- across the OE or skin from seawater teleost fish mummichog (Degnan et al., 1977) and *Gillichthys mirabilis* skin (Marshall, 1981) when saline bathed both sides of the epithelium. To test asymmetrical conditions, isotonic saline on the mucosal side was replaced by full-strength SW and, to test hypersaline conditions, 2SW on the mucosal side. Solution changes were flow through, adding the new solution to the bottom of the chamber while aspirating from the top; complete exchange was accomplished by flow through of 10× the chamber volume. With asymmetrical solutions, the V_t was adjusted for any diffusion potential, measured with no epithelium in the aperture and with nylon mesh instead. Asymmetry potentials were less than 1 mV with Cortland's on one side and SW or 2SW on the other side. V_t and R were monitored; I_{sc} under asymmetrical conditions is complicated by diffusion potentials, no longer represents Cl^- secretion rate and was not recorded.

Electrophysiology theory

The Nernst equation predicts for systems that are permeable to one ion:

$$\Delta\psi = \frac{RT}{z_i F}\ln\left[\frac{a_i C_i^o}{a_i C_i^i}\right], \quad (1)$$

where the transmembrane voltage ($\Delta\psi$) is generated in asymmetrical conditions and C_i^o is the concentration on the outside and C_i^i is the concentration on the inside, R=8.3143 Coul. V/K mol, F=96,494 Coul mol^{-1} equiv and z_i is the valence. Because salt solutions above 0.1 mol l^{-1} are non-ideal, we apply the empirically derived activity coefficient (a_i) to describe the degree of dissociation of the salt (NaCl principally) (Robinson and Stokes, 1959). Although no biological system is uniquely permeable to one ion species, this relationship for the Na^+ gradient (E_{Na}) approximates the voltage against which marine fish must secrete Na^+, assuming that Na^+ moves via a simple barrier to diffusion.

Leak conductance (G_L) was calculated as an extrapolation of the epithelial conductance (G_t) versus I_{sc} adapted from a previous method (Kültz and Onken, 1993), but instead of using the spontaneous variation of G_t and I_{sc}, the epithelia in Ussing chambers were inhibited by application of hypotonic shock (60 mOsm kg^{-1} reduction of basolateral and apical bathing solutions), a treatment that rapidly inhibits the transcellular pathway of active ion secretion by dephosphorylation of NKCC and CFTR (Marshall et al., 2009, 2005).

Pharmaceuticals

To test for the presence of membrane rafts in the apical membrane of ionocytes, we added drugs to inhibit the operation of dynamin and caveolin, two major endo- and exocytosis effectors (Ares and Ortiz, 2012; Bajmoczi et al., 2009). Chlorpromazine, a dynamin 1 and dynamin 2 inhibitor (and Ca^{2+} calmodulin inhibitor) (Ares and Ortiz, 2012), was added stepwise from 1.0 to 50 µmol l^{-1} to the mucosal side of paired OE in symmetrical Cortland's saline, one serving as a time control and the test side receiving the drug. Changes in I_{sc}, V_t and R_t were measured for at least 30 min before the drug was rinsed off the OE. Similarly, filipin, a disruptor of caveolin-1 operation and a cholesterol sequestration drug, was added at 1.53 µmol l^{-1} to the apical side of the OE, incubated for up to 1 hour, when the OE were challenged with hypotonic shock (80% diluted Cortland's saline, both sides) and the responses compared with paired time control OE.

Plasma ions and osmolality

Plasma ion concentration was measured by ion chromatography (Dionex DX 500, Sunnyvale, CA, USA). Plasma from animals acclimated to SW and 2SW was centrifuged for 5 min at 14,000 r.p.m., 10 µl of plasma was diluted to 1 ml and duplicate samples of 25 µl measured with 0.5 ml injections used to ensure complete rinsing between samples. Conductance (µS) readout was interpolated from a linear plot of standard NaCl or KCl solutions multiplied by the dilution factor (100). Plasma osmolality was measured by vapor pressure osmometry (Wescor model 5520, Logan, UT, USA); readings were interpolated from osmometry standards provided by the manufacturer.

Statistical analyses

Data are expressed as means±s.e.m. Significant difference for apical crypt depths was determined by a two-way analysis of variance (ANOVA) followed by Tukey's multiple comparison *a posteriori* tests. Fisher's exact test was performed to analyze nominal data of CFTR distribution in the apical crypts (condensed versus diffuse). Node distribution differences and plasma osmolality and ions were compared using unpaired two-tailed *t*-tests. Significant difference was ascribed if P<0.05.

Acknowledgements

Many thanks to StFX animal care facility for expert animal care and to the helpful suggestions of the reviewers.

Competing interests

The authors declare no competing or financial interests.

Author contributions

Conception and design: R.R.F.C. and W.S.M. equally. Execution of experiments: electron microscopy, G.N.R.; electrophysiology, G.M.M.Z., L.N.C., M.S.; immunocytochemistry, R.R.F.C., K.L.G., M.S. Data interpretation and writing of the manuscript: R.R.F.C., W.S.M., L.N.C., G.N.R. Revisions: W.S.M., R.R.F.C., G.N.R.

Funding

This work was supported by a Natural Sciences and Engineering Research Council Discovery grant [RGPIN3698-2009 to W.S.M.], a Chaisson Scholarship to L.N.C., an Irving Mentorship to K.L.G. and a University Council Research Grant 2013-47 to W.S.M.

References

Ares, G. R. and Ortiz, P. A. (2012). Dynamin 2, clathrin, and lipid rafts mediate endocytosis of the apical Na/K/2Cl cotransporter NKCC2 in thick ascending limbs. *J. Biol. Chem.* **287**, 37824-37834.

Avella, M., Pärt, P. and Ehrenfeld, J. (1999). Regulation of Cl^- secretion in seawater fish (*Dicentrarchus labrax*) gill respiratory cells in primary culture. *J. Physiol.* **516**, 353-363.

Bagherie-Lachidan, M., Wright, S. I. and Kelly, S. P. (2008). Claudin-3 tight junction proteins in *Tetraodon nigroviridis*: cloning, tissue-specific expression, and a role in hydromineral balance. *Am. J. Physiol. Regul. Integr. Comp. Physiol.* **294**, R1638-R1647.

Bagherie-Lachidan, M., Wright, S. I. and Kelly, S. P. (2009). Claudin-8 and -27 tight junction proteins in puffer fish *Tetraodon nigroviridis* acclimated to freshwater and seawater. *J. Comp. Physiol. B Sys. Environ. Physiol.* **179**, 419-431.

Bajmoczi, M., Gadjeva, M., Alper, S. L., Pier, G. B. and Golan, D. E. (2009). Cystic fibrosis transmembrane conductance regulator and caveolin-1 regulate epithelial

cell internalization of *Pseudomonas aeruginosa*. *Am. J. Physiol. Cell Physiol.* **297**, C263-C277.
Bradbury, N., Clark, J., Watkins, S., Widnell, C., Smith, H. and Bridges, R. (1999). Characterization of the internalization pathways for the cystic fibrosis transmembrane conductance regulator. *Am. J. Physiol. Lung Cell. Mol. Physiol.* **276**, L659-L668.
Bui, P., Bagherie-Lachidan, M. and Kelly, S. P. (2010). Cortisol differentially alters claudin isoforms in cultured puffer fish gill epithelia. *Mol. Cell. Endocrinol.* **317**, 120-126.
Burnett, K. G., Bain, L. J., Baldwin, W. S., Callard, G. V., Cohen, S., Di Giulio, R. T., Evans, D. H., Gomez-Chiarri, M., Hahn, M. E., Hoover, C. A. et al. (2007). *Fundulus* as the premier teleost model in environmental biology: opportunities for new insights using genomics. *Comp. Biochem. Physiol. D Genom. Proteom.* **2**, 257-286.
Chambers, V. C. (1973). The use of ruthenium red in an electron microscope study of cytophagocytosis. *J. Cell Biol.* **57**, 874-878.
Chasiotis, H. and Kelly, S. P. (2011). Permeability properties and occludin expression in a primary cultured model gill epithelium from the stenohaline freshwater goldfish. *J. Comp. Physiol. B Biochem. Syst. Environ. Physiol.* **181**, 487-500.
Chasiotis, H., Kolosov, D., Bui, P. and Kelly, S. P. (2012). Tight junctions, tight junction proteins and paracellular permeability across the gill epithelium of fishes: a review. *Respir. Physiol. Neurobiol.* **184**, 269-281.
Choe, K. P., Havird, J., Rose, R., Hyndman, K., Piermarini, P. and Evans, D. H. (2006). COX2 in a euryhaline teleost, *Fundulus heteroclitus*: primary sequence, distribution, localization, and potential function in gills during salinity acclimation. *J. Exp. Biol.* **209**, 1696-1708.
Cioni, C., De Merich, D., Cataldi, E. and Cataudella, S. (1991). Fine structure of chloride cells in freshwater and seawater adapted *Oreochromis niloticus* (Linnaeus) and *Oreochromis mossambicus* (Peters). *J. Fish Biol.* **39**, 197-209.
Degnan, K. J. (1984). The sodium and chloride dependence of chloride secretion by the opercular epithelium. *J. Exp. Zool.* **231**, 11-17.
Degnan, K. J. and Zadunaisky, J. A. (1980). Passive sodium movements across the opercular epithelium: the paracellular shunt pathway and ionic conductance. *J. Membr. Biol.* **55**, 175-185.
Degnan, K. J., Karnaky, K. J. and Zadunaisky, J. A. (1977). Active chloride transport in the *in vitro* opercular skin of a teleost (*Fundulus heteroclitus*), a gill-like epithelium rich in chloride cells. *J. Physiol.* **271**, 155-191.
Epstein, F. H., Katz, A. I. and Pickford, G. E. (1967). Sodium- and potassium-activated adenosine triphosphatase of gills: role in adaptation of teleosts to salt water. *Science* **156**, 1245-1247.
Eriksson, Ö. and Wistrand, P. J. (1986). Chloride transport inhibition by various types of 'loop' diuretics in fish opercular epithelium. *Acta Physiol. Scand.* **126**, 93-101.
Evans, D. H., Piermarini, P. M. and Choe, K. P. (2005). The multifunctional fish gill: dominant site of gas exchange, osmoregulation, acid-base regulation, and excretion of nitrogenous waste. *Physiol. Rev.* **85**, 97-177.
Fletcher, C. R. (1977). Potential dependence of sodium fluxes across the gills of marine teleosts. *J. Comp. Physiol. B* **117**, 277-289.
Foskett, J. K. and Machen, T. E. (1985). Vibrating probe analysis of teleost opercular epithelium: correlation between active transport and leak pathways of individual chloride cells. *J. Membr. Biol.* **85**, 25-35.
Foskett, J. K., Hubbard, G. M., Machen, T. E. and Bern, H. A. (1982). Effects of epinephrine, glucagon and vasoactive intestinal polypeptide on chloride secretion by teleost opercular membrane. *J. Comp. Physiol. B.* **146**, 27-34.
Griffith, R. W. (1974). Environment and salinity tolerance in the genus *Fundulus*. *Copeia* **1974**, 319-331.
Guggino, W. B. (1980). Salt balance in embryos of *Fundulus heteroclitus* and *F. bermudae* adapted to seawater. *Am. J. Physiol. Reg. Integ. Comp. Physiol.* **238**, R42-R49.
Haas, M. and Forbush, B. (2000). The Na-K-Cl cotransporter of secretory epithelia. *Annu. Rev. Physiol.* **62**, 515-534.
Haggie, P. M., Stanton, B. A. and Verkman, A. S. (2004). Increased diffusional mobility of CFTR at the plasma membrane after deletion of its C-terminal PDZ binding motif. *J. Biol. Chem.* **279**, 5494-5500.
Hiroi, J., McCormick, S., Ohtani-Kaneko, R. and Kaneko, T. (2005). Functional classification of mitochondrion-rich cells in euryhaline Mozambique tilapia (*Oreochromis mossambicus*) embryos, by means of triple immunofluorescence staining for Na^+/K^+-ATPase, Na^+/K^+/2Cl cotransporter and CFTR anion channel. *J. Exp. Biol.* **208**, 2023-2036.
Hootman, S. R. and Philpott, C. W. (1980). Accessory cells in teleost branchial epithelium. *Am. J. Physiol. Regul. Integr. Comp. Physiol.* **238**, R199-R206.
Hwang, P. P. and Hirano, R. (1985). Effects of environmental salinity on intercellular organization and junctional structure of chloride cells in early stages of teleost development. *J. Exp. Zool.* **236**, 115-126.
Karnaky, K. J. J. (1980). Ion-secreting epithelia: chloride cells in the head region of *Fundulus heteroclitus*. *Am. J. Physiol. Regul. Integr. Comp. Physiol.* **238**, R185-R198.
Karnaky, K. J. J. (1986). Structure and function of the chloride cell of *Fundulus heteroclitus* and other teleosts. *Am. Zool.* **26**, 209-224.
Karnaky, K. J., Jr (1991). Teleost osmoregulation: changes in the tight junction in response to the salinity of the environment. In *The Tight Junction* (ed. M. Cereijido), pp. 175-185. Boca Raton, USA: CRC Press.
Karnaky, K. J. and Kinter, W. B. (1977). Killifish opercular skin: a flat epithelium with a high density of chloride cells. *J. Exp. Zool.* **199**, 355-364.
Karnaky, K. J., Jr, Kinter, L. B., Kinter, W. B. and Stirling, C. E. (1976). Teleost chloride cell. II Autoradiographic localization of gill Na^+, K^+-ATPase in killifish (*Fundulus heteroclitus*) adapted to low and high salinity environments. *J. Cell Biol.* **70**, 157-177.
Kelly, S. P. and Wood, C. M. (2002). Cultured gill epithelia from freshwater tilapia (*Oreochromis niloticus*): effect of cortisol and homologous serum supplements from stressed and unstressed fish. *J. Membr. Biol.* **190**, 29-42.
Keys, A. and Willmer, E. N. (1932). 'Chloride secreting cells' in the gills of fishes, with special reference to the common eel. *J. Physiol.* **76**, 368-378.
Kültz, D. and Onken, H. (1993). Long-term acclimation of the teleost *Oreochromis mossambicus*to various salinities: two different strategies in mastering hypertonic stress. *Mar. Biol.* **117**, 527-533.
Kültz, D., Li, J., Gardell, A. and Sacchi, R. (2013). Quantitative molecular phenotyping of gill remodeling in a cichlid fish responding to salinity stress. *Mol. Cell. Proteom.* **12**, 3962-3975.
Laverty, G. and Skadhauge, E. (2012). Adaptation of teleosts to very high salinity. *Comp. Biochem. Physiol. A Mol. Integr. Physiol.* **163**, 1-6.
Mancera, J. M. and McCormick, S. D. (2000). Rapid activation of gill Na^+, K^+-ATPase in the euryhaline teleost *Fundulus heteroclitus*. *J. Exp. Zool.* **287**, 263-274.
Marshall, W. S. (1981). Sodium dependency of active chloride transport across isolated fish skin (*Gillichthys mirabilis)*. *J. Physiol.* **319**, 165-178.
Marshall, W. S. (1985). Paracellular ion transport in trout opercular epithelium models osmoregulatory effects of acid precipitation. *Can. J. Zool.* **63**, 1816-1822.
Marshall, W. S. (2002). Na+, Cl^-, Ca^{2+} and Zn^{2+} transport by fish gills: retrospective review and prospective synthesis. *J. Exp. Zool.* **293**, 264-283.
Marshall, W. S. and Bern, H. A. (1980). Ion transport across the isolated skin of the teleost *Gillichthys mirabilis*. In *Epithelial Transport in the Lower Vertebrates* (ed. B. Lahlou), pp. 337-350. Cambridge: Cambridge University Press.
Marshall, W. S., Bryson, S. E. and Garg, D. (1993). Alpha-2-adrenergic inhibition of Cl^- transport by opercular epithelium is mediated by intracellular Ca^{2+}. *Proc. Natl. Acad. Sci. USA* **90**, 5504-5508.
Marshall, W. S., Bryson, S. E., Midelfart, A. and Hamilton, W. F. (1995). Low-conductance anion channel activated by cAMP in teleost Cl^--secreting cells. *Am. J. Physiol. Regul. Integr. Comp. Physiol.* **268**, R963-R969.
Marshall, W. S., Emberley, T. R., Singer, T. D., Bryson, S. E. and McCormick, S. D. (1999). Time course of salinity adaptation in a strongly euryhaline estuarine teleost, *Fundulus heteroclitus*: a multivariable approach. *J. Exp. Biol.* **202**, 1535-1544.
Marshall, W. S., Lynch, E. A. and Cozzi, R. R. F. (2002). Redistribution of immunofluorescence of CFTR anion channel and NKCC cotransporter in chloride cells during adaptation of the killifish *Fundulus heteroclitus* to sea water. *J. Exp. Biol.* **205**, 1265-1273.
Marshall, W. S., Ossum, C. G. and Hoffmann, E. K. (2005). Hypotonic shock mediation by p38 MAPK, JNK, PKC, FAK, OSR1 and SPAK in osmosensing chloride secreting cells of killifish opercular epithelium. *J. Exp. Biol.* **208**, 1063-1077.
Marshall, W. S., Watters, K. D., Hovdestad, L. R., Cozzi, R. R. F. and Katoh, F. (2009). CFTR Cl^- channel functional regulation by phosphorylation of focal adhesion kinase at tyrosine 407 in osmosensitive ion transporting mitochondria rich cells of euryhaline killifish. *J. Exp. Biol.* **212**, 2365-2377.
McCormick, S. D., Sundell, K., Björnsson, B. T., Brown, C. L. and Hiroi, J. (2003). Influence of salinity on the localization of Na^+/K^+-ATPase, $Na^+/K^+/2Cl^-$ cotransporter (NKCC) and CFTR anion channel in chloride cells of the Hawaiian goby (*Stenogobius hawaiiensis*). *J. Exp. Biol.* **206**, 4575-4583.
McCormick, S. D., Regish, A. M. and Christensen, A. K. (2009). Distinct freshwater and seawater isoforms of Na^+/K^+-ATPase in gill chloride cells of Atlantic salmon. *J. Exp. Biol.* **212**, 3994-4001.
Monteiro, S. M., Oliveira, E., Fontainhas-Fernandes, A. and Sousa, M. (2010). Fine structure of the branchial epithelium in the teleost *Oreochromis niloticus*. *J. Morphol.* **271**, 621-633.
Philpott, C. W. and Copeland, D. E. (1963). Fine structure of chloride cells from three species of *Fundulus*. *J. Cell Biol.* **18**, 389-404.
Pic, P. (1978). A comparative study of the mechanism of Na^+ and Cl^- excretion by the gill of *Mugil capito* and *Fundulus heteroclitus*: effects of stress. *J. Comp. Physiol. B.* **123**, 155-162.
Potts, W. T. W. (1984). Transepithelial potentials in fish gills. In *Fish Physiology Volume X Gills Part B* (ed. W. S. Hoar and D. J. Randall), pp. 105-128. New York: Academic Press.
Riedel, R., Caskey, L. and Costa-Pierce, B. A. (2002). Fish biology and fisheries ecology of the Salton Sea, California. *Hydrobiologia* **473**, 229-244.
Robertson, J. C. and Hazel, J. R. (1999). Influence of temperature and membrane lipid composition on the osmotic water permeability of teleost gills. *Physiol. Biochem. Zool.* **72**, 623-632.

Robinson, R. A. and Stokes, R. H. (1959). *Electrolyte Solutions*. 2nd edn, p. 389. London: Butterworth.

Sardella, B., Matey, V., Cooper, J., Gonzalez, R. and Brauner, C. (2004). Physiological, biochemical and morphological indicators of osmoregulatory stress in 'California' Mozambique tilapia (*Oreochromis mossambicus* x *O.* urolepis hornorum) exposed to hypersaline water. *J. Exp. Biol.* **207**, 1399-1413.

Sardella, B. A., Kültz, D., Cech, J. J., Jr and Brauner, C. J. (2008). Salinity-dependent changes in Na^+/K^+-ATPase content of mitochondria-rich cells contribute to differences in thermal tolerance of Mozambique tilapia. *J. Comp. Physiol. B Biochem. Syst. Environ. Physiol.* **178**, 249-256.

Sardet, C., Pisam, M. and Maetz, J. (1979). The surface epithelium of teleostean fish gills. cellular and junctional adaptations of the chloride cell in relation to salt adaptation. *J. Cell. Biol.* **80**, 96-117.

Scheffey, C., Foskett, J. K. and Machen, T. E. (1983). Localization of ionic pathways in the teleost opercular membrane by extracellular recording with a vibrating probe. *J. Membr. Biol.* **75**, 193-203.

Scott, G. R. and Schulte, P. M. (2005). Intraspecific variation in gene expression after seawater transfer in gills of the euryhaline killifish *Fundulus heteroclitus*. *Comp. Biochem. Physiol. A Mol. Integr. Physiol.* **141**, 176-182.

Semple, J. W., Green, H. J. and Schulte, P. M. (2002). Molecular cloning and characterization of two Na/K-ATPase isoforms in *Fundulus heteroclitus*. *Mar. Biotechnol.* **4**, 512-519.

Shen, W.-P., Horng, J.-L. and Lin, L.-Y. (2011). Functional plasticity of mitochondrion-rich cells in the skin of euryhaline medaka larvae (*Oryzias latipes*) subjected to salinity changes. *Am. J. Physiol. Regul. Integr. Comp. Physiol.* **300**, R858-R868.

Shiraishi, K., Kaneko, T., Hasegawa, S. and Hirano, T. (1997). Development of multicellular complexes of chloride cells in the yolk-sac membrane of tilapia (*Oreochromis mossambicus*) embryos and larvae in seawater. *Cell Tissue Res.* **288**, 583-590.

Silva, P., Solomon, R., Spokes, K. and Epstein, F. H. (1977a). Ouabain inhibition of gill Na-K-ATPase: relationship to active chloride transport. *J. Exp. Zool.* **199**, 419-426.

Silva, P., Stoff, J., Field, M., Fine, L., Forrest, J. N. and Epstein, F. H. (1977b). Mechanism of active chloride secretion by shark rectal gland: role of Na^+,K^+-ATPase in chloride transport. *Am. J. Physiol. Renal Physiol.* **233**, F298-F306.

Singer, T. D., Tucker, S. J., Marshall, W. S. and Higgins, C. F. (1998). A divergent CFTR homologue: highly regulated salt transport in the euryhaline teleost *F.* heteroclitus. *Am. J. Physiol. Cell Physiol.* **274**, C715-C723.

Singer, T. D., Keir, K. R., Hinton, M., Scott, G. R., McKinley, R. S. and Schulte, P. M. (2008). Structure and regulation of the cystic fibrosis transmembrane conductance regulator (CFTR) gene in killifish: a comparative genomics approach. *Comp. Biochem. Physiol. D Genom. Proteom.* **3**, 172-185.

Tang, C. H. and Lee, T. H. (2007). The effect of environmental salinity on the protein expression of Na^+/K^+-ATPase, $Na^+/K^+/2Cl^-$ cotransporter, cystic fibrosis transmembrane conductance regulator, anion, exchanger 1, and chloride channel 3 in gills of a euryhaline teleost, Tetraodon nigroviridis. *Comp. Biochem. Physiol. A Mol. Integr. Physiol.* **147**, 521-528.

Tipsmark, C. K., Kiilerich, P., Nilsen, T. O., Ebbesson, L. O. E., Stefansson, S. O. and Madsen, S. S. (2008a). Branchial expression patterns of claudin isoforms in Atlantic salmon during seawater acclimation and smoltification. *Am. J. Physiol. Regul. Integr. Comp. Physiol.* **294**, R1563-R1574.

Tipsmark, C. K., Baltzegar, D. A., Ozden, O., Grubb, B. J. and Borski, R. J. (2008b). Salinity regulates claudin mRNA and protein expression in the teleost gill. *Am. J. Physiol. Regul. Integr. Comp. Physiol.* **294**, R1004-R1014.

Towle, D. W., Gilman, M. E. and Hempel, J. D. (1977). Rapid modulation of gill Na^++K^+-dependent ATPase activity during acclimation of the killifish *Fundulus heteroclitus* to salinity change. *J. Exp. Zool.* **202**, 179-185.

Varsamos, S., Diaz, J. P., Charmantier, G., Flik, G., Blasco, C. and Connes, R. (2002). Branchial chloride cells in sea bass (*Dicentrarchus labrax*) adapted to fresh water, seawater, and doubly concentrated seawater. *J. Exp. Zool.* **293**, 12-26.

Whitehead, A. (2010). The evolutionary radiation of diverse osmotolerant physiologies in killifish (*Fundulus sp.*). *Evolution* **64**, 2070-2085.

Whitehead, A., Galvez, F., Zhang, S., Williams, L. M. and Oleksiak, M. F. (2011a). Functional genomics of physiological plasticity and local adaptation in killifish. *J. Hered.* **102**, 499-511.

Whitehead, A., Roach, J. L., Zhang, S. and Galvez, F. (2011b). Genomic mechanisms of evolved physiological plasticity in killifish distributed along an environmental salinity gradient. *Proc. Natl. Acad. Sci. USA* **108**, 6193-6198.

Whitehead, A., Pilcher, W., Champlin, D. and Nacci, D. (2012). Common mechanism underlies repeated evolution of extreme pollution tolerance. *Proc. R. Soc. B Biol. Sci.* **279**, 427-433.

Wood, C. M. and Grosell, M. (2008). A critical analysis of transepithelial potential in intact killifish (*Fundulus heteroclitus*) subjected to acute and chronic changes in salinity. *J. Comp. Physiol. B Biochem. Syst. Environ. Physiol.* **178**, 713-727.

Wood, C. M. and Marshall, W. S. (1994). Ion balance, acid-base regulation, and chloride cell function in the common killifish, *Fundulus heteroclitus*: a euryhaline estuarine teleost. *Estuaries* **17**, 34-52.

Wood, C. M., Gilmour, K. M. and Pärt, P. (1998). Passive and active transport properties of a gill model, the cultured branchial epithelium of the freshwater rainbow trout (*Oncorhynchus mykiss*). *Comp. Biochem. Physiol. A Mol. Integr. Physiol.* **119**, 87-96.